

Relevance of Correlated Hopping in Mixed Valence Phenomena within Extended Falicov–Kimball Model

Piyali Ghosh¹, Nanda Kumar Ghosh¹✉, Subhadip Nath²

¹Department of Physics, University of Kalyani, Kalyani-741235, West Bengal, India

²Department of Physics, Krishnagar Government College, Krishnagar-741101, India

Received 21 July 2025

Abstract. The effect of correlated hopping of d -electrons between Nearest-Neighbor (NN) sites on Mixed-Valent systems has been studied with the theoretical support of extended Falicov-Kimball model (EFKM). Both the thermodynamic and ground state properties have been investigated through the exact diagonalization method. The f -electron density $\langle n_i^f \rangle$ decreases with the f -level energy (E) showing valence transition. The maximum coulomb correlation is seen for lower correlated hopping interaction (K). The specific heat curves show sharp single-peak structure. However, for higher values of f -level energy E , an inclination to double-peak structure is observed at higher temperatures (T). The system becomes more disordered with the increase of hopping value.

KEY WORDS: Mixed valence compound, Extended Falicov–Kimball model, Correlated hopping interaction, Exact diagonalization method, Valence transition.

1 Introduction

A significant number of rare earth compounds (such as SmS, SmB₆, SmSe, SmTe etc.) exhibit mixed valence phenomena [1]. In rare-earth compounds, the outermost shell configuration is $(4f)^n(sd)^m$. When pressure or temperature is applied, the f -level energy E rises, causing the $4f$ shell to become unstable. As a consequence of fact, two valence states $(4f)^n(sd)^m$ and $(4f)^{n-1}(sd)^{m+1}$ coexist with one another in some rare-earth compounds, that's why these compounds are known as mixed valence (MV) compounds. The average number of f -electrons per site becomes non-integral in value, and the f -level electrons take on a partially band-like character. Therefore, the characteristics of mixed-valent compounds are anomalous due to the non-integral valence [2]. Rare-earth compounds have a wide range of uses in contemporary society because of

2 Relevance of Correlated Hopping in Mixed Valence Phenomena within...

their unique characteristics. Many computer components, including CD-ROM, hard drive, and DVD, are built of rare-earth magnets. The refining process of petroleum uses catalysts based on lanthanum. In the field of cancer treatment, particularly in cancer diagnostics and therapy, rare-earth compounds have been used in one of the most unexpected ways [3].

The ratio of two ions, Sm^{2+} and Sm^{3+} in a homogeneous mixed-valence compound, such as SmB_6 is 4:6. The ionic configuration of samarium is an admixture of $4f^6$ and $4f^5$ given with a $5d$ defined and localized electron, according to numerous investigations on SmB_6 [4–7]. Actually, due to the electronic configuration of rare-earth elements, some rare earth compounds exhibit MV as well as superconducting properties [8–13].

Both theoretical and experimental research was done on the different anomalous features of MV compounds. To explain how different interactions affect the characteristics of MV compounds, numerous models and techniques have been employed. Two peaks in the X-ray L_{III} absorption edge spectra of samarium hexaboride (SmB_6) support the mixed valence property of samarium [7, 14]. Many intensive experimental studies have been carried out to understand MV phenomena [15]. The anomalous properties of MV systems are revealed by numerous measurements of temperature dependence of resistance [16], low temperature specific heat [17], magnetoresistance [18], electronic specific heat coefficient [19], and other MV compounds.

The magnetic characteristics of rare-earth tetraborides are studied in [20] by extending the Ising model with the first, second, third, and fourth nearest-neighbor spin couplings using the Monte Carlo approach. The density functional theory (DFT) is used in [21] to examine the electronic characteristics of rare-earth compounds SmB_6 . Furthermore, a numerical investigation on rare-earth tetraborides is conducted utilizing the FKM combined with the Ising model [22]. Research on the FKM is still being conducted utilizing various methods. The effect of external magnetic field on the stability of the excitonic phase due to local hybridization is studied using the density-matrix-renormalization-group (DMRG) approach in the one-dimensional spin-1/2 Falicov-Kimball model [23]. Calculations based on Hartree-Fock approximation (HFA) with charge-density-wave (CDW) instability have been performed to explore the ground state properties of the spinless FKM expanded by f -electron hopping and nonlocal hybridization with inversion symmetry in two and three dimensions [24]. The EFKM has been examined at half-filling within the HFA (for different crystal lattices) and the results are compared with the rigorous ones generated inside the dynamical mean field theory (DMFT) [25]. The DMRG technique is used to investigate the impact of various parameters on the stability of charge and spin-order in the spin-one-half FKM with the Ising-type Hund coupling [26]. The magnetization process in the case of rare-earth tetraborides is detailed for the spin-electron model utilizing both the exact diagonalization and Quantum Monte Carlo analysis [27]. A study on the effect of charge stripes on rare-earth tetraboride magnetization processes was conducted in [28].

MV compounds exhibit a variety of interactions that extend the traditional FKM [29]. Correlated hopping [30], electron-phonon interaction [31–33], nonlocal Coulomb interaction [34], next-nearest-neighbor (*NNN*) hopping [35], *NNN* Coulomb interaction [36], next-to-next-nearest-neighbor hopping [37], pseudo-hybridization interaction [38], doping induced valence transition [39] and so on are already well-studied. Experimental measurements of the mixed-valent CeNi₄Cr compound's temperature dependency of heat capacity have been made [40]. Yet, an exact technique is used to examine the ground state phase diagram of the extended Hubbard model with nearest and next-to-nearest neighbor interactions at its ground state [41]. But, the impact of density dependent correlated hopping interaction on mixed-valent systems within FKM is not studied properly.

So, the central importance of our present study is the effect of the correlated hopping in mixed-valent systems studied in 2D square lattice with 8-sites with the support of FKM. Valence transitions as well as thermodynamic properties have been studied using exact diagonalization method. However, in a finite size cluster contained in a self-consistent host that represents the rest of the system, finite size effects cannot be disregarded. Only nearest-neighbor (*NN*) sites are taken into consideration in this case. Furthermore, no computation taking into account long-range correlations where the finite size effect dominates, has been performed. As a result, the findings here can, at least qualitatively, establish the behaviour of rare-earth MV compounds.

2 Hamiltonian and Formulation

This study considers the cluster of a 2D square lattice with 8 sites and two bands. The Hamiltonian taken into consideration in this work is

$$H = H_0 + H', \quad (1)$$

where

$$H_0 = E \sum_{i\sigma} f_{i\sigma}^\dagger f_{i\sigma} + U \sum_i f_{i\uparrow}^\dagger f_{i\uparrow} f_{i\downarrow}^\dagger f_{i\downarrow} + G \sum_{i\sigma\sigma'} f_{i\sigma}^\dagger f_{i\sigma} d_{i\sigma'}^\dagger d_{i\sigma'} + V \sum_{\langle i,j \rangle \sigma} (f_{i\sigma}^\dagger d_{j\sigma} + d_{j\sigma}^\dagger f_{i\sigma}) - t \sum_{\langle i,j \rangle \sigma} d_{i\sigma}^\dagger d_{j\sigma}, \quad (2)$$

$$H' = K \sum_{i,j,\sigma} d_{i\sigma}^\dagger d_{j\sigma} (f_{i,-\sigma}^\dagger f_{i,-\sigma} + f_{j,-\sigma}^\dagger f_{j,-\sigma}). \quad (3)$$

Here, on the 2D square lattice, *i* and *j* sites are all pairs of nearest neighbors; $f_{i\sigma}^\dagger$ and $f_{i\sigma}$ represent the creation and annihilation operators for localized *f*-electrons at lattice site *i* with spin σ , and $d_{i\sigma}^\dagger$, $d_{i\sigma}$ for itinerant *d*-electrons with spin σ respectively. *E* stands for *f*-level energy; *U* is the on-site Coulomb interaction between *f*-electrons with opposite spins at site *i*; *G* represents the on-site

4 Relevance of Correlated Hopping in Mixed Valence Phenomena within...

Coulomb interaction between f and d electrons; V represents the f - d hybridization interaction; t is the hopping of d -electrons between nearest neighbour sites. The correlated hopping interaction is represented by H' .

The basis states under consideration, as determined on eight-site, have the following form [38]:

$$|n_{1\uparrow}^f n_{1\downarrow}^f n_{1\uparrow}^d n_{1\downarrow}^d n_{2\uparrow}^f n_{2\downarrow}^f n_{2\uparrow}^d n_{2\downarrow}^d \cdots n_{8\uparrow}^f n_{8\downarrow}^f n_{8\uparrow}^d n_{8\downarrow}^d\rangle. \quad (4)$$

According to Eq. (4), the basis vectors are linearly combined to give the eigenvectors of H .

The f -electron density is

$$\langle n_i^f \rangle = \frac{1}{N} \sum_{\sigma} f_{i\sigma}^{\dagger} f_{i\sigma}, \quad (5)$$

where N represents the number of lattice sites in this context.

Inter-site f - d correlation function is

$$C_{fd} = \langle f_{i\sigma}^{\dagger} d_{j\sigma} \rangle. \quad (6)$$

The on-site f - d correlation function is

$$C_d^f = \langle n_{i\sigma}^f n_{i\sigma'}^d \rangle = \langle f_{i\sigma}^{\dagger} f_{i\sigma} d_{i\sigma'}^{\dagger} d_{i\sigma'} \rangle. \quad (7)$$

Entropy per lattice site is

$$S = \frac{1}{N} \left(k_B \ln Z + \frac{\langle H \rangle}{T} \right). \quad (8)$$

Temperature-dependent specific heat is

$$C = k_B \beta^2 \frac{\partial^2}{\partial \beta^2} \ln Z, \quad (9)$$

where

$$Z = \sum_a e^{-\beta E_a},$$

over all basis states, the total partition function is computed, the corresponding eigenvalues are with eigenvalues E_a 's and $\beta = \frac{1}{k_B T}$, k_B is the Boltzmann constant. Throughout our current investigation, k_B is assumed to be one.

3 Results and Discussions

Two electrons are taken into account in this communication. The values of the parameters used in this paper are taken from the results of various experimental observations.

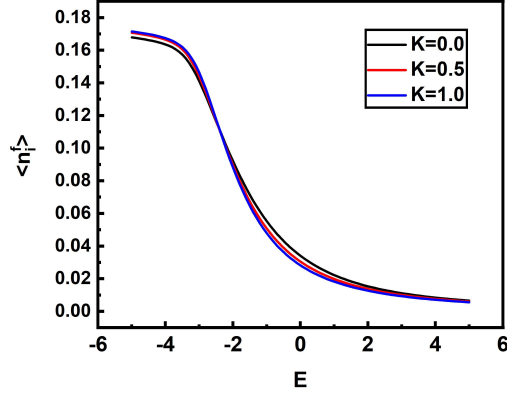


Figure 1. Variation of f -electron density $\langle n_i^f \rangle$ with E for distinct values of K . Here $U = 5.0$, $G = 1.0$, $V = 0.5$, $t = 1.0$.

The value of the f -electron density decreases from a maximum value with increasing value of f -level energy E (Figure 1). The maximum value of $\langle n_i^f \rangle$ from which it starts to decrease is different for different values of correlated hopping of d -electrons, which is perturbed by the f -electron density with opposite spin at the NN sites. The first-order valence transition occurs at a critical value of $E = E_c$ [42]. E_c is the same for all graphs for distinct values of correlated hopping interaction (K). The valence transition is sharper for higher values of correlated hopping terms (K). $\langle n_i^f \rangle$ becomes almost saturated near the zero value despite the increasing value of E .

The value of the inter-site f - d correlation function (C_{fd}) is shown in Figure 2.

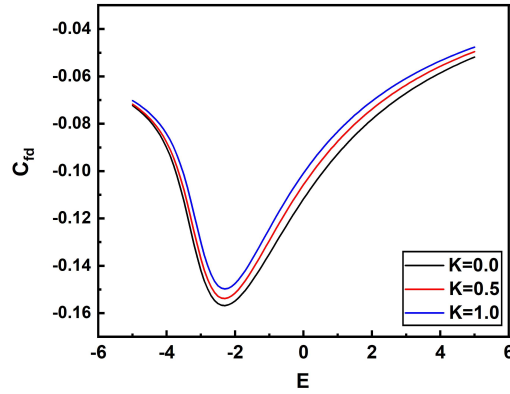


Figure 2. Inter-site f - d correlation function C_{fd} vs. E curves for distinct values of K . Here $U = 5.0$, $G = 1.0$, $V = 0.5$, $t = 1.0$.

6 Relevance of Correlated Hopping in Mixed Valence Phenomena within...

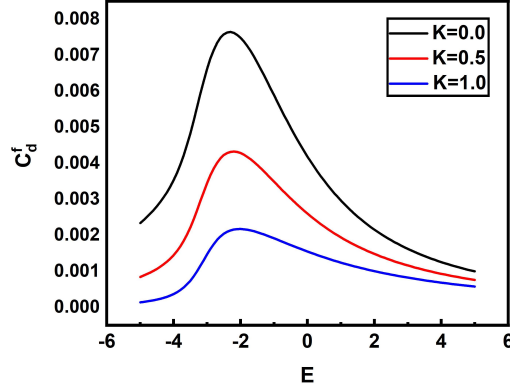


Figure 3. On-site $f - d$ correlation C_d^f versus f -level energy E for different K . Here $U = 5.0$, $G = 1.0$, $V = 0.5$, $t = 1.0$.

The correlation decreases with increasing value of E up to a critical E , that is, E_c . E_c is different for different graphs indicating different values of correlated hopping. Attaining E_c , it further increases with E . For metallic or insulating state, the correlated function approaches a value close to zero [43]. In the insulating phase for smaller E (negative) or at higher E value (positive) the correlation is near equal to zero. This figure is in agreement with Figure 1.

Figure 3 shows the variation of on-site $f - d$ coulomb correlation function with E for various values of K . The value of correlation is maximum in the vicinity at the energy $E = E_c$. But the maximum coulomb correlation is seen for lower values of correlated hopping interaction. It appears that correlated hopping interaction destroys the uniform distribution of f - and d -electrons [41]. With the increase of E , the f -electrons are shifted to d -electron orbitals due to valence transition (Figure 1). It appears that there is a symmetry of numbers of f - and d -electrons at $E = E_c$. Hence, we get a maximum of the correlation. At lower or higher values of E (in the insulating or metallic phase) the correlation decreases.

Figure 4 depicts the characteristics of variation of entropy per lattice site S with temperature T . At any particular temperature, entropy S increases with K . Therefore, K induces disorder in the system. It implies the significance of correlated hopping in MV phenomena. The deviation between the curves becomes more pronounced as the temperature rises, peaking around $0.25 < T < 1.0$. This temperature range is known as the transition temperature region [44], and the condition associated with the valence fluctuation is indicated by the maximum entropy at $K = 1.0$. For $T \geq 1.0$, good convergence is seen.

Figure 5 shows the characteristics of specific heat variation with temperature for different correlated hopping interaction K . The curves show single-peak structure at low temperature region. The peak-height decreases with K indicating a

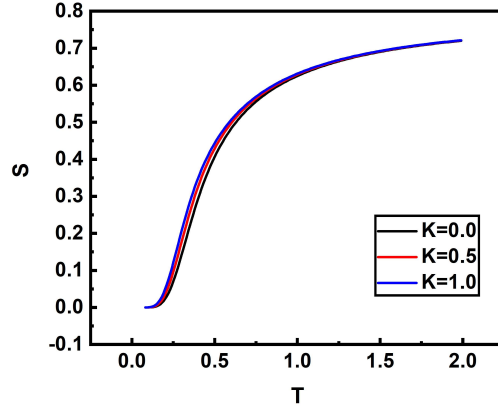


Figure 4. Temperature variation of entropy for distinct values of K . Here $E = -2.0$, $U = 5.0$, $G = 1.0$, $V = 0.5$, $t = 1.0$.

decrease in effective energy. The appearance of this sharp peak is caused by the large number of many body states which is degenerate with the ground state.

Comparing these results with our previous findings, it is apparent that correlated hopping and pseudo-hybridization behave oppositely. Figure 6 represents temperature variation of specific heat for different f -level energy E at a correlated hopping strength $K = 0.5$. For $E < -2.0$, tendency to double-peak structure appears [45]. This wide peak at higher temperature is caused by the Schottky effect [46]. With the increase of the magnitude of f -level energy, the peak-height decreases and shifts to lower temperature region. Comparing the characteristics

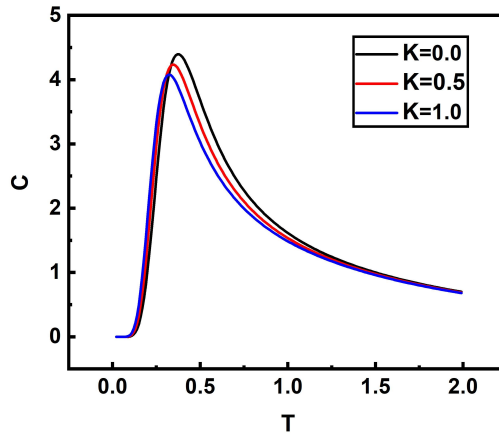


Figure 5. Variation of specific heat (C) with T for distinct values of K . Here $E = -2.0$, $U = 5.0$, $G = 1.0$, $V = 0.5$, $t = 1.0$.

8 Relevance of Correlated Hopping in Mixed Valence Phenomena within...

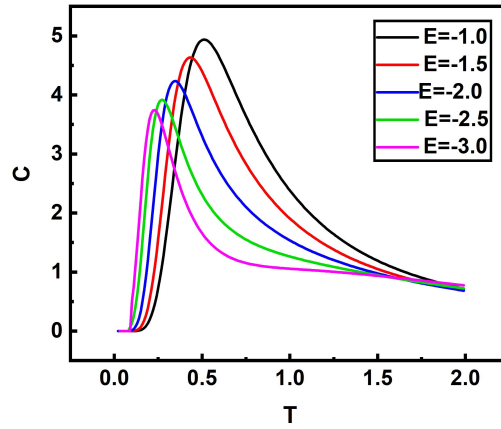


Figure 6. Graph of specific heat with temperature for different values of E . Here $U = 5.0$, $G = 1.0$, $V = 0.5$, $t = 1.0$, $K = 0.5$.

with the previous results [38], it can be concluded that K decreases the peak-height, i.e., the effective energy of the system.

4 Conclusion

Summarizing, the present study on the relevance of correlated hopping (K) in MV phenomena has established that valence transition is sharper for enhanced values of K . The symmetry of f - and d -electrons at $E = E_c$ is broken due to the presence of K . Entropy curves show that K induces disorder in the system. The specific heat curves show single-peak structure. However, a tendency to double-peak structure appears at higher values of K (Schottky effect). This hopping also decreases the effective energy of the system. The results clearly indicate the relevance of correlated hopping in mixed valence phenomena.

Acknowledgement

We are grateful to the University of Kalyani for the infrastructural support. The work was financially supported by the Faculty Research Grant (FRG 2024-2025) of the University of Kalyani.

References

- [1] C.M. Varma (1976) Mixed-valence compounds. *Rev. Mod. Phys.* **48** 219-238.
- [2] J.M. Robinson (1979) Valence transitions and intermediate valence states in rare earth and actinide materials. *Phys. Rep.* **51** 1-62.

- [3] J. Wang, S. Li (2022) Applications of rare earth elements in cancer: Evidence mapping and scientometric analysis. *Front. Med.* **9** 2282-2294.
- [4] zonno2024 M. Zonno, et al. (2024) Mixed-valence state in the dilute-impurity regime of La-substituted SmB_6 . *Nat. Commun.* **15**(1) 7621.
- [5] J.N. Chazalviel, M. Campagna, G.K. Wertheim, P.H. Schmidt (1976) Configurational mixing and 4f-photoemission lineshapes in SmB_6 . *Solid State Commun.* **19** 725-728.
- [6] R.L. Cohen, M. Eibschütz, K.W. West (1970) Electronic and Magnetic Structure of SmB_6 . *Phys. Rev. Lett.* **24** 383-386.
- [7] M. Mizumaki, S. Tsutsui, F. Iga (2009) Temperature dependence of Sm valence in SmB_6 studied by X-ray absorption spectroscopy. *J. Phys.: Conf. Ser.* **176** 012034-012038.
- [8] C.F. Ratto, B. Coqblin, E.G. d'Agliano (1969) Superconductivity of lanthanum and cerium at high pressures. *Adv. Phys.* **18** 489-513.
- [9] S. Gabani, K. Flachbart, K. Siemensmeyer, T. Mori (2020) Magnetism and superconductivity of rare earth borides. *J. Alloys Compd.* **821** 153201-153250.
- [10] D. Johrendt (2020) Rare earth based superconducting materials. In: *Rare Earth Chemistry*, eds. R. Pöttgen, T. Jüstel, C.A. Strassert. De Gruyter STEM, pp. 557-575.
- [11] W. Chen, et al. (2023) Enhancement of superconducting properties in the La–Ce–H system at moderate pressures. *Nat. Commun.* **14**(1) 2660.
- [12] W. Chen, et al. (2020) Superconductivity and equation of state of lanthanum at megabar pressures. *Phys. Rev. B* **102**(13) 134510.
- [13] G.S. Wang, et al. (2025) Insights into the structure and superconductivity of lanthanum under high-pressure. *Vacuum* **233** 113898.
- [14] E. Mijit, et al. (2024) Temperature and pressure dependencies of Sm valence in (SmB_6) Kondo insulator probed by X-ray absorption spectroscopy. *Phys. Rev. B* **689** 416174.
- [15] J.M. Lawrence, P.S. Riseborough, R.D. Parks (1981) Valence fluctuation phenomena. *Rep. Prog. Phys.* **44** 1-85.
- [16] A. Menth, E. Buehler, T.H. Geballe (1969) Magnetic and semiconducting properties of (SmB_6). *Phys. Rev. Lett.* **22** 295-297.
- [17] L.J. Sundström (1978) Low temperature heat capacity of the rare earth metals. *Handbook on the physics and chemistry of rare earths* **1** 379-410.
- [18] H. Hartmann, et al. (2005) Magnetoresistance, specific heat and magnetocaloric effect of equiatomic rare-earth transition-metal magnesium compounds. *J. Phys.: Condens. Matter* **17** 7731-7742.
- [19] K. Sato, Y. Isikawa, K. Mori (1992) Magnetic specific heat of light rare earth Heusler compounds RInCu_2 (R=La, Ce, Pr, Nd and Sm). *J. Magn. Magn. Mater.* **104** 1435-1436.
- [20] H. Čenčariková, P. Farkašovský (2015) Fractional magnetization plateaus in the extended Ising model on the Shastry–Sutherland lattice: Application to rare-earth metal tetraborides. *Phys. Status Solidi (b)* **252** 333-338.
- [21] M. Gmitra, H. Čenčariková, P. Farkašovský (2014) First-Principles Study of Kondo Insulator SmB_6 . *Acta Phys. Pol. A* **126** 298-299.

10 Relevance of Correlated Hopping in Mixed Valence Phenomena within...

- [22] P. Farkašovský, H. Čenčariková, S. Mat'áš (2010) Numerical study of magnetization processes in rare-earth tetraborides. *Phys. Rev. B* **82** 054409.
- [23] P. Farkašovský (2024) Influence of magnetic field on the electronic ferroelectricity in the external Falicov–Kimball model. *J. Phys.: Condens. Matter* **36** 085601.
- [24] P. Farkašovský (2023) Hartree-Fock exploration of electronic ferroelectricity, valence transitions, and metal-insulator transitions in the extended Falicov–Kimball model. *Phys. Rev. B* **108** 075161.
- [25] K.J. Kapcia, R. Lemański, M.J. Zygmunt (2020) Extended Falicov–Kimball model: Hartree–Fock vs DMFT approach. *J. Phys.: Condens. Matter* **33**(6) 065602.
- [26] P. Farkašovský (2023) On the stability of charge and spin order in the spin-one-half Falicov–Kimball model with the Ising-type Hund coupling. *J. Magn. Magn. Mater.* **573** 170659.
- [27] P. Farkašovský, L. Regeciová (2020) Formation of Magnetization Plateaus in Rare Earth Tetraborides: Exact Diagonalization and Quantum Monte Carlo Studies. *J. Supercond. Nov. Magn.* **33** 3463–3467.
- [28] P. Farkašovský (2025) Impact of charge stripes on magnetization processes in rare-earth tetraborides. *J. Magn. Magn. Mater.* **629** 173284.
- [29] L.M. Falicov, J.C. Kimball (1969) Simple model for semiconductor-metal transitions: SmB_6 and transition-metal oxides. *Phys. Rev. Lett.* **22** 997–999.
- [30] N.K. Ghosh, S.K. Bhowmick, N.S. Mondal (2011) Role of correlated hopping in mixed valence phenomena. *Pramana - J. Phys.* **76** 139–147.
- [31] N.K. Ghosh, S.C. Ghosh, R.L. Sarkar (1990) Electron–Phonon Interaction Induced Hybridisation in Mixed-Valence Systems. *phys. status solidi (b)* **158** 223–228.
- [32] S.C. Ghosh, N.K. Ghosh, R.L. Sarkar (1990) Role of Electron–Phonon Interaction Induced Hybridisation in Spin Included Mixed-Valence Phenomena. *phys. status solidi (b)* **161** 661–666.
- [33] S.K. Bhowmick, N.K. Ghosh (2011) Falicov–Kimball model extended by electron-phonon interaction (EPI). *Armen. J. Phys.* **4** 30–37.
- [34] P. Farkašovský (2019) The influence of nonlocal interactions on valence transitions and formation of excitonic bound states in the generalized Falicov–Kimball model. *Eur. Phys. J. B* **92** 1–5.
- [35] S.K. Bhowmick, N.K. Ghosh (2012) Falicov–Kimball model extended by next-nearest–neighbor (NNN) hopping of d-electrons. *Indian J. Phys.* **86** 345–349.
- [36] P. Mukherjee, N.K. Ghosh (2018) Impact of NNN Coulomb Interaction on the Properties of Mixed Valence Compounds. *Int. J. Curr. Trends Sci. Technol.* **8** 20195–20202.
- [37] P. Ghosh, N.K. Ghosh (2022) Effect of next to next-nearest-neighbor (NNNN) hopping interaction in mixed valence systems and study of the thermodynamic properties. *IOP Conf. Ser.: Mater. Sci. Eng.* **1258** 012005.
- [38] P. Ghosh, N.K. Ghosh (2025) Effect of Pseudo-Hybridization Interaction on Ground State and Finite Temperature Properties of Mixed Valence Systems. *Bulg. J. Phys.* **52** 99–109.
- [39] P. Ghosh, N.K. Ghosh (2025) Doping Induced Valence Transition in Mixed Valence Systems. *IJONS* **16** 92619–92623.
- [40] M. Zapotokova, M. Reiffers (2022) CeNi_4Cr compounds and its thermodynamic properties. *J. of Phys.: Conf. Ser.* **2164** 012055–012059.

- [41] Z. Szabó (1999) Improved stability regions for ground states of the extended Hubbard model. *Phys. Rev. B* **59**(15) 10007.
- [42] H. Čenčariková, P. Farkašovský, M. Žonda (2008) The influence of nonlocal coulomb interaction on ground-state properties of the Falicov–Kimball model in one and two dimensions. *Int. J. Mod. Phys. B* **22** 2473-2487.
- [43] S.K. Bhowmick, N.K. Ghosh (2012) Nonlocal Coulomb interaction in the two-dimensional spin-1/2 Falicov–Kimball model. *Pramana – J. Phys.* **78** 289-296.
- [44] N.S. Mondal, N.K. Ghosh (2010) Role of next-nearest-neighbour hopping in the internal structure of the ground state and finite temperature quantities of 2D t - J model. *Pramana – J. Phys.* **74** 1009-1015.
- [45] N.K. Ghosh, S.C. Ghosh, R.L. Sarkar (1992) Studies on Some Ground State Properties and Specific Heat of Mixed-Valence Systems. *phys. stat. sol. (b)* **171** 107-112.
- [46] D. Mazumdar, K. Das, I. Das (2021) Schottky-like anomaly in the heat capacity and magnetocaloric effect of charge-ordered single-crystalline (Sm, Ca, Sr) MnO_3 compound. *J. Magn. Magn. Mater.* **540** 168447 (1-10).